The DOI for this manuscript is doi: 10.1175/BAMS-D-15-00035.1

The final published version of this manuscript will replace the preliminary version at the above DOI once it is available.

If you would like to cite this EOR in a separate work, please use the following full citation:

Scott, J., M. Alexander, D. Murray, D. Swales, and J. Eischeid, 2015: The Climate Change Web Portal: a system to access and display climate and earth system model output from the CMIP5 archive. Bull. Amer. Meteor. Soc. doi:10.1175/BAMS-D-15-00035.1, in press.

The Climate Change Web Portal: A System to Access and Display Climate and Earth System Model Output from the CMIP5 archive.

James D Scott[1,2], Michael A Alexander[2], Donald R Murray[1,2], Dustin Swales[1,2] and Jon Eischeid[1,2]

1 Cooperative Institute for Research in Environmental Sciences, University of Colorado, Boulder, CO

2 NOAA/Earth System Research Laboratory, Boulder, CO

Corresponding Author Address:

James Scott
NOAA Earth System Research Laboratory
R/PSD1
325 Broadway, Boulder, CO 80305-3328
Email: james.d.scott@noaa.gov

Motivation

The way in which the climate changes in response to increases in anthropogenic greenhouse gases is one of the foremost questions for the scientific community, policy makers and the general public. A key approach for examining climate, especially how it will change in the future, uses complex computer models that include atmosphere, ocean, sea ice and land components. Some models also simulate additional facets of the earth system, including marine chemistry and biology. Model simulations indicate that temperatures have warmed over the past century, and will continue to rise into the future due to greenhouse gas forcing (IPCC, 2014). However, the very large number of model simulations, the sheer volume of data they have generated, and output that might not be directly relevant for many applications can make it extremely difficult for potential users to access, view and evaluate the data.

While useful web tools exist for viewing model-simulated climate change including the "Climate Reanalyzer", "Climate Wizard", "National Climate Change Viewer", "KNMI Climate Change Atlas" and "Climate Variability and Diagnostics Package", the Climate Change Web Portal offers some unique capabilities, including examination of model bias, inter-model variability, changes in variance, ocean physical and biogeochemical model output.

The Climate Change Web Portal (http://www.esrl.noaa.gov/psd/ipcc/) was developed by the NOAA/ESRL Physical Sciences Division to access and display the large volumes of climate and earth system model output from the Coupled Model Inter-comparison Project Version 5 (CMIP5, Taylor et al. 2012, van Vuuren et al. 2011) that informed the recently released Intergovernmental Panel on Climate Change (IPCC) report. The portal has two components that encompass *i)* land and rivers or *ii)* oceans and marine ecosystems. Recent changes in Federal agency directives and programmatic mandates require Federal managers to consider climate change in water resources and environmental planning. As a result, resource managers are now required to make judgments regarding which aspects of climate projection information are applicable to a given decision, including decisions to modify system operations, invest in new or improved infrastructure, and establish long-term management objectives. The web portal provides scientists, resource managers, and stakeholders a framework to evaluate and interpret the models by comparing them to observations (land/rivers portion) during the historic record and view how they project climate change in the future. To this end, Federal water and fisheries managers have already used this tool in decision making processes. The goal of this manuscript is to introduce the reader to the capabilities of the web portal.

Methods and Examples

By pre-processing the model output and utilizing a number of software tools, the web-portal allows users to quickly display maps and time series via a series of menu options. As a first step, output from the CMIP5 models, which have different horizontal resolutions, are interpolated to a 1° lat-lon grid to allow for inter-model comparisons. Statistics for different climate metrics are then computed on the common grid. A combination of software languages including Javascript, Python and NCAR's Command Language (NCL), are used to access the NetCDF files to generate an image in real time. From the portal, set of menus allows the user to choose: *i*) an individual model or the model ensemble mean; *ii*) an experiment (i.e.,past or future greenhouse gas forcing); *iii*) fields to display such as precipitation and ocean temperature at 100 m depth; *iv*) statistics, such as the mean, median, 90 percentile (%), for the land component and standardized anomalies for the ocean component; *v*) annual mean or three-month seasons; *vi*) time periods in the 20th and 21st century, and *vii*) pre-defined or a user-defined region. Once the menus choices are selected, either four maps or two time series are displayed.

We illustrate the features of the system via examples of the land/river and ocean components of the portal. The first example (Fig. 1) shows the 90th percentile of the surface air temperature (SAT, °C) during JJA for the years 1911-2005 (the SAT of the 10th warmest summer in each grid square over the 95-year period) over North America from *i*) observations (University of Delaware Terrestrial Air Temperature, upper left) and *ii*) the ensemble mean of the CMIP5 models (upper right), *iii*) the difference between the two, indicating the model bias (lower left) and *iv*) the difference between the 90% SAT in the RCP 8.5 experiment during the 21st century (2006-2100) minus the values in the historical period (1911-2005), indicating the climate change signal (lower right). The ensemble model mean generally matches the observed pattern of very warm summer seasons, where the 90% exceeds 25°C over the southwest US and the southern Great Plains, with values less than 20°C over the Rocky Mountains and northwest US. However, on average the models are too warm, by approximately 0.5°-2°C, over most of the Great Plains but slightly cooler than observed over the southeast US. The bias has a complex pattern over Mexico and the western US due in part to the smoothed representation of mountains in climate models. SAT extremes in JJA are more likely over the entire domain in the 21st century relative to the 20th, especially away from the coasts where the change in the 90% exceeds 5°C between 35° and 55°N.

The web portal can also be used to examine time varying changes. For example, the 30-year running mean of observed and simulated precipitation (mm) over the entire year for the New England watershed or Hydrologic Unit Code (HUC, a hierarchical representation of river basins) is presented in Fig. 2. In general the models simulate more precipitation over New England during the 20th century than observed (GPCC version 5), although the observed values are within the full range of the CMIP5 models (left panel). The right panel shows the observed and simulated precipitation values with their respective means over the 1901-2005 period removed ("anomaly"). Both observations and the models indicate an increase in precipitation for New England. While the spread in the precipitation increases among the models towards the end of the 21st century, all model simulations indicate an increase in precipitation by 2100. Enhanced precipitation, which is especially prominent in winter (not shown), could lead to increased flooding when the snow melts in late winter/early spring.

Due to the absence of adequate observations for some ocean fields, the plots for the ocean component of the web portal are based solely on the climate model output. The annual and ensemble mean 0-700 m heat content (J m^{-2}) in the North Pacific Ocean is shown in Fig. 3, including the: *i)* mean during the historical period (1956-2005) (upper left), *ii)* mean climate change signal given by the heat content in 2006-2055 minus 1956-2005 (upper right), *iii)* year-to-year variability as indicated by the standard deviation during the historical period (lower left) and *iv)* ratio of the interannual variance in the future relative to the historical period (lower right). The mean heat content is relatively high in the subtropics and low in high latitude with a tight gradient in between at ~40°N especially in the western side of the basin. The heat content is indicative of the wind driven upper ocean circulation with subtropical and subpolar gyres and the Kuroshio/Oyashio Extension current along the tight gradient between them. The latter is a region of enhanced interannual variability relative to the rest of the North Pacific Ocean. The difference between periods indicates that the heat content of the entire North Pacific increases in the first half of the 21st century. However, the increase is not uniform but is concentrated along 40°N in the western Pacific, suggesting either a northward shift of the Kuroshio/Oyashio current extension and/or an increase in the surface heat flux into the ocean or an increase convergence of heat near the front (Wu et al. 2012). Finally, the interannual heat content variability decreases during 2006-2055 relative to 1956-2005 over most of the North Pacific except at ~45°N, just north of the front during the 20th century.

Annual average sea surface salinity (SSS) fields over the North Atlantic as simulated by NCAR's Community Climate System model, version 4 (CCSM4, Gent et al. 2011) are shown in Fig. 4. The climatological mean SSS during 1956-2005 exhibits a maximum (> 36 psu) in the subtropics and the Mediterranean, with higher values in the western Atlantic and minimum values (< 33 psu) over most of the Arctic Ocean. The CCSM4 indicates that SSS will increase in the subtropics and decrease north of ~40°N in the 21st relative to the 20th century. The standard deviation of SSS is maximized in the northwest Atlantic near 40°N, at the boundary between the salty subtropical and relatively fresh subpolar gyres, and in the vicinity of the sea ice edge that extends from north of Iceland northeastward to Svalbard. The 21st/20th century SSS standard deviation is positive over most of the Atlantic north of 30°N suggesting that salinity variability will increase over much of the North Atlantic in the future especially between Iceland and Great Britain.

Earth system models in the CMIP5 archive simulate aspects of the biogeochemistry in the ocean, including primary production by phytoplankton that grow via the uptake of carbon and other inorganic molecules using energy provided by sunlight. Generally marine ecosystem models simulate several classes of phytoplankton, although the number of kinds of that are represented differ between models. The annual average primary production from all phytoplankton classes over the upper 150 m is shown for the Arctic and subpolar oceans (> 50°N) in Fig. 5. In the historical period, average 1956-2005, the North Atlantic, North Pacific and Bering Sea are very productive, while the central Arctic is not. Several factors influence primary productivity including light, and temperature, which are limiting at high latitudes, and nutrients, which limit phytoplankton growth in midlatitudes and the tropics. The primary productivity during the historical period indicates that conditions are conducive for phytoplankton growth during spring through fall in subpolar regions but ice cover, cold temperatures and long periods without sunlight, limit the annual production in the central Arctic and on both sides of Greenland. Productivity is enhanced north of Europe where warm water from the Atlantic enters the Arctic Ocean. The climate change signal (2050-2099 minus 1956-2005) exhibits reduced primary productivity over the North Atlantic and Gulf of Alaska and increased productivity in the Arctic, the Sea of Okhotsk and most of the Bering Sea. The largest increase in productivity in the Arctic coincides with the largest decrease in sea ice (not shown), which enables more light to reach the ocean allowing for more photosynthesis. The decrease in productivity in the North Atlantic and Gulf of Alaska may result from an increase in stratification, due to a freshening and warming near the surface (see Capotondi et al. 2012), which reduces the amount of nutrients mixed into the upper ocean from deeper ocean.

Summary

While the Climate Change web-portal was initially designed for hydrologic and fishery applications, we anticipate that it will be useful to a wide range of users. To that end, we have included additional information including tutorials and metadata accessible through help links on the portal. In addition, the derived fields used to make the plots can be downloaded as a netCDF file, so users can use their own software package to create plots. The portal is designed so that more variables, experiments, statistics, and features can be added in the future. Currently there are some capabilities such as comparing models side by side, comparing ocean model output with observations and comparing the variability of the climate change signal among all the models that are not possible. We plan to add these features and enhance web-portal tutorials in the future. We feel that this tool provides a useful framework for users to assess current and future changes in CMIP5 climate simulations. More details on climate modeling, the IPCC report, the CMIP5 experiments and observational datasets can be found here: http://www.esrl.noaa.gov/psd/ipcc/references.htm.

Acknowledgements

We thank Levi Brekke, Jeff Arnold, and Roger Griffis for the encouragement and providing financial support through the Bureau of Reclamation, Army Corps of

Engineers and NOAA’s National Marine Fishery Service through the acknowledge (SMECC) program, respectively.

References

Capotondi, A., M. Alexander, N. Bond, E. Curchitser, and J. Scott, 2012: Enhanced Upper-Ocean Stratification with Climate Change in the CMIP3 Models. *J. Geophs Res. - Oceans*, **117**, C04031, doi:10.1029/2011JC007409.

Gent, P. R., G. Danabasoglu, L. J. Donner, M. M. Holland, E. C. Hunke, S. R. Jayne, D. M. Lawrence, R. B. Neale, P. J. Rasch, M. Vertenstein, P. H. Worley, Z. -L. Yang, and M. Zhang, 2011: The Community Climate System Model Version 4. *J. Climate*, **24** (19), 4973-4991.

IPCC, 2014: Summary for Policymakers. In: Climate Change 2014: Impacts, Adaptation, and Vulnerability. Part A: Global and Sectoral Aspects. Contribution of Working Group II to the Fifth Assessment Report of the Intergovernmental Panel on Climate Change [Field, C.B., V.R. Barros, D.J. Dokken, K.J. Mach, M.D. Mastrandrea, T.E. Bilir, M. Chatterjee, K.L. Ebi, Y.O. Estrada, R.C. Genova, B. Girma, E.S. Kissel, A.N. Levy, S. MacCracken, P.R. Mastrandrea, and L.L. White (eds.)]. Cambridge University Press, Cambridge, United Kingdom and New York, NY, USA, pp. 1-32. PDF

Taylor, K.E., R.J. Stouffer, G.A. Meehl: 2012: An Overview of CMIP5 and the experiment design. *Bull. Amer. Meteor. Soc.*, **93**, 485-498, doi:10.1175/BAMS-D-11-00094.1

van Vuuren, Detlef P., et al. 2011: The representative concentration pathways: an overview. *Climate Change*, **109**, 1-2, pp. 5-31, doi: 10.1007/s10584-011-0148-z

Wu, L., W. Cai, L. Zhang, H. Nakamura, A. Timmermann, T. Joyce, M. J. McPhaden, M. Alexander, B. Qiu, M. Visbeck, P. Chang, and B. Giese, 2012: Enhanced warming over the global subtropical western boundary currents. *Nature Climate Change*. DOI: 10.1038/NCLIMATE1353.

Figure Captions

Fig.1: Snapshot from the Land and Rivers section of the Climate Change Web Portal depicting the 90th percentile of Jun-Jul-Aug (JJA) seasonal mean near surface air temperature (SAT, °C) for the years 1911-2005 from i) observations (University of Delaware Terrestrial Air Temperature, upper left) and ii) the ensemble mean of the CMIP 5 models (upper right), *iii*) the difference between the two, indicating the model bias (lower left) and *iv*) the difference between the 90% SAT in the RCP 8.5 experiment during the 21st century (2006-2100) minus the values in the historical period (1911-2005), (lower right).

Fig.2: 30-year running mean precipitation time series for area average precipitation (mm year^{-1}) in the New England watershed (HUC) for mean values (left) and anomaly values obtained by removing the 1901-2005 climatology from both the observations and the individual model simulation s(right). GPCC observations are in black, the CMIP5 ensemble mean is in red, and gray shading represents the entire CMIP5 model range (light gray), 10th-90th percentile range (darker gray) and the 25th-75th percentile range (darkest gray).

Fig.3: Snapshot from the Ocean and Marine Ecosystems section of the Climate Change Web Portal depicting the CMIP5 ensemble mean Ocean Heat Content integrated over the top 700 m (J m^{-2}) for *i)* mean during the historical period (1956-2005) (upper left), *ii)* mean climate change signal from the RCP8.5 scenarios: 2006-2055 minus the 1956-2005 period in the historical experiments (upper right), *iii)* year-to-year variability as indicated by the standard deviation during the historical period (lower left) and *iv)* ratio of the interannual variance in the future relative to the historical period (lower right); presented as ratio rather than the difference of the variances as the former is used to test for significance via the F-test.

Fig.4: Snapshot from the Ocean and Marine Ecosystems section of the Climate Change Web Portal depicting the CMIP5 ensemble mean Sea Surface Salinity (PSU) for *i)* mean during the historical period (1956-2005) (upper left), *ii)* mean climate change signal from the RCP8.5 scenarios: 2050-2099 minus the 1956-2005 period in the historical experiments (upper right), *iii)* year-to-year variability as indicated by the standard deviation during the historical period (lower left) and *iv)* ratio of the interannual variance in the future relative to the historical period (lower right).

Fig.5: Snapshot from the Ocean and Marine Ecosystems section of the Climate Change Web Portal depicting the CMIP5 ensemble mean Net Primary Productivity of Carbon by Phytoplankton in the top 150m (1e^{-9} mol m^{-2} s^{-1}) for *i)* mean during the historical period (1956-2005) (upper left), *ii)* mean climate change signal from the RCP8.5 scenarios: 2050-2099 minus the 1956-2005 period in the historical experiments (upper right), *iii)* year-to-year variability as indicated by the standard deviation during the historical period (lower left) and *iv)* ratio of the interannual variance in the future relative to the historical period (lower right).

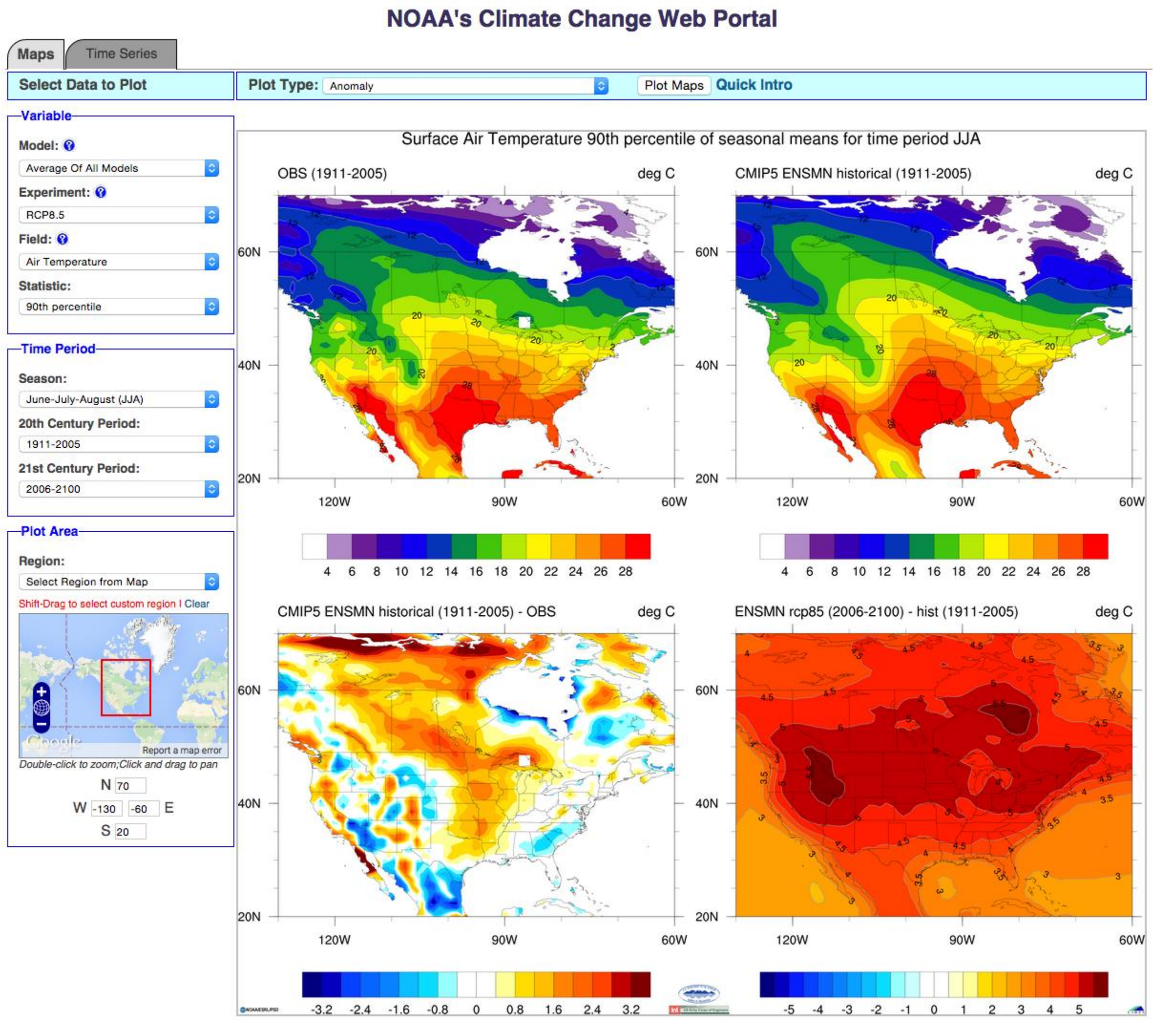

Fig.1: Snapshot from the Land and Rivers section of the Climate Change Web Portal depicting the 90th percentile of Jun-Jul-Aug (JJA) seasonal mean near surface air temperature (SAT, °C) for the years 1911-2005 from i) observations (University of Delaware Terrestrial Air Temperature, upper left) and ii) the ensemble mean of the CMIP 5 models (upper right), *iii*) the difference between the two, indicating the model bias (lower left) and *iv*) the difference between the 90% SAT in the RCP 8.5 experiment during the 21st century (2006-2100) minus the values in the historical period (1911-2005), (lower right).

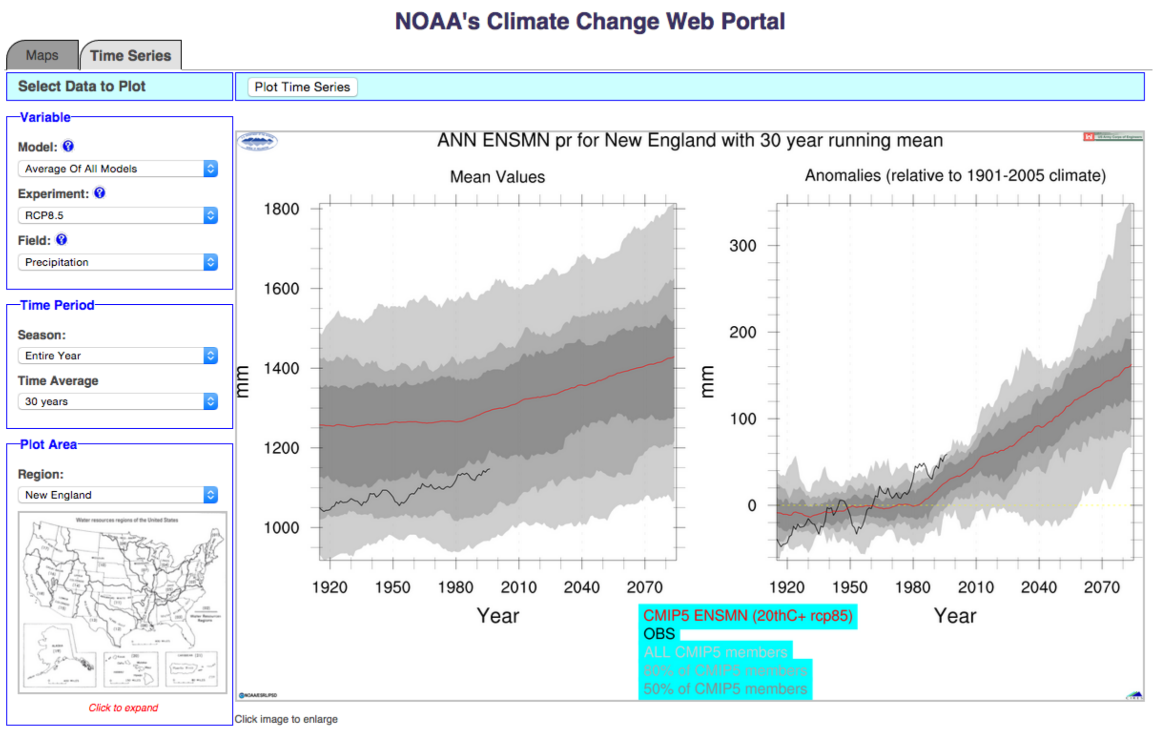

Fig.2: 30-year running mean precipitation time series for area average precipitation (mm year^{-1}) in the New England watershed (HUC) for mean values (left) and anomaly values obtained by removing the 1901-2005 climatology from both the observations and the individual model simulation s(right). GPCC observations are in black, the CMIP5 ensemble mean is in red, and gray shading represents the entire CMIP5 model range (light gray), 10th-90th percentile range (darker gray) and the 25th-75th percentile range (darkest gray).

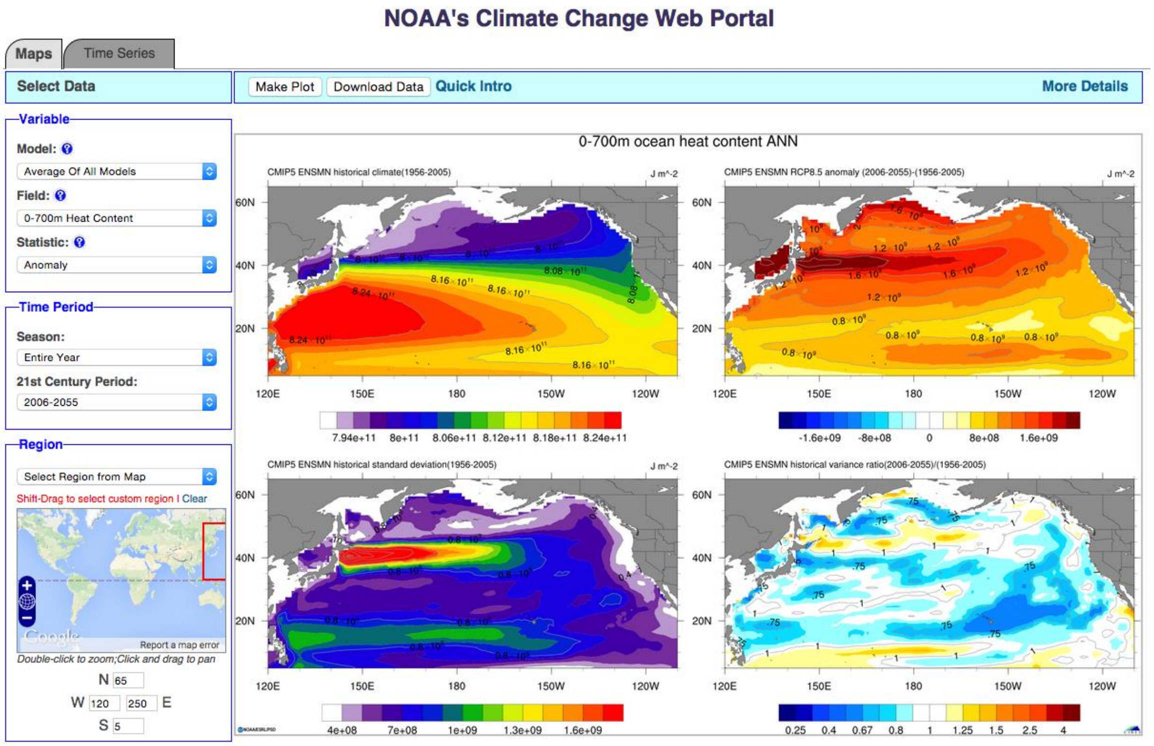

Fig.3: Snapshot from the Ocean and Marine Ecosystems section of the Climate Change Web Portal depicting the CMIP5 ensemble mean Ocean Heat Content integrated over the top 700 m ($J\ m^{-2}$) for *i)* mean during the historical period (1956-2005) (upper left), *ii)* mean climate change signal from the RCP8.5 scenarios: 2006-2055 minus the 1956-2005 period in the historical experiments (upper right), *iii)* year-to-year variability as indicated by the standard deviation during the historical period (lower left) and *iv)* ratio of the interannual variance in the future relative to the historical period (lower right); presented as ratio rather than the difference of the variances as the former is used to test for significance via the F-test.

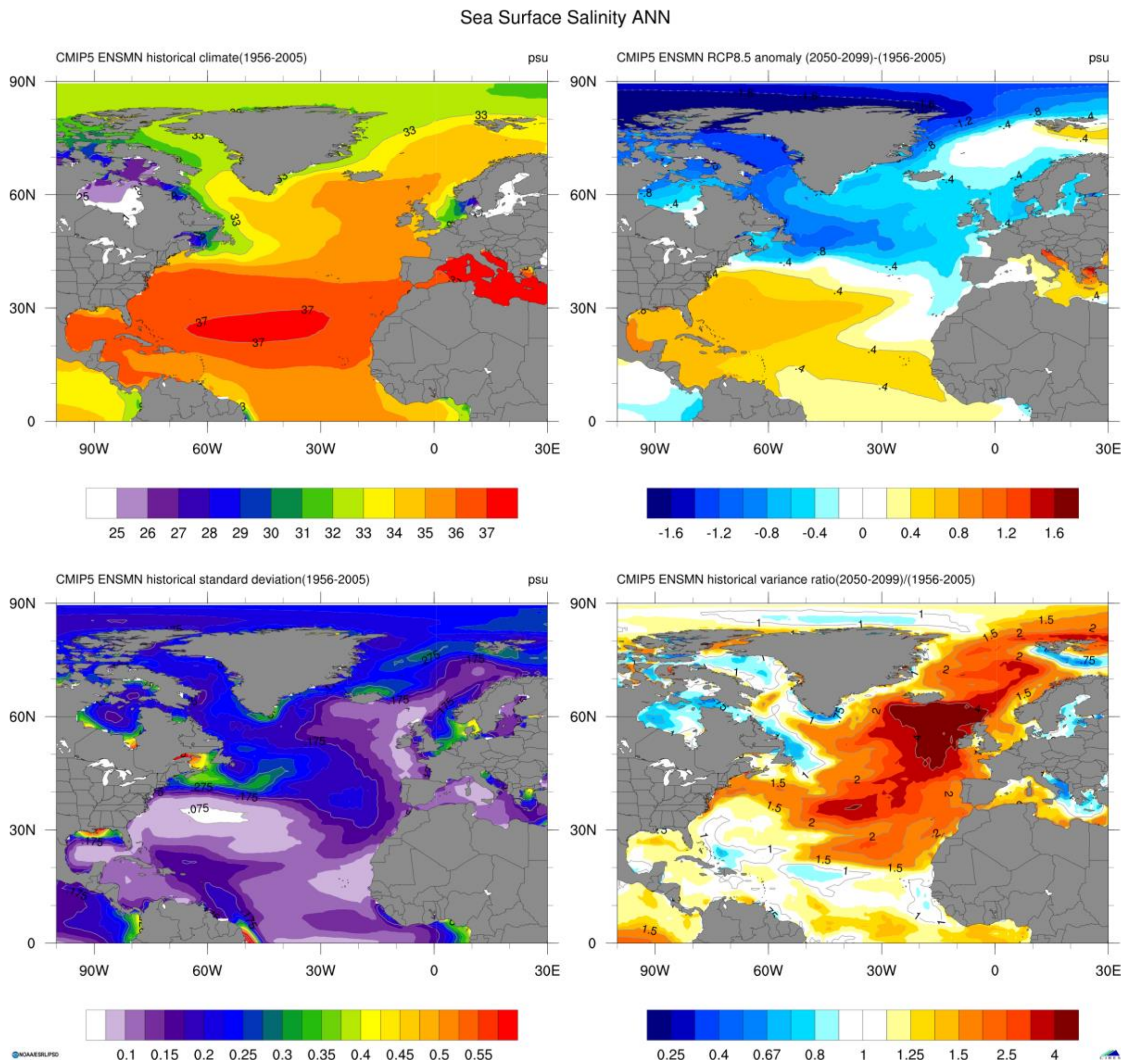

Fig.4: Snapshot from the Ocean and Marine Ecosystems section of the Climate Change Web Portal depicting the CMIP5 ensemble mean Sea Surface Salinity (PSU) for *i)* mean during the historical period (1956-2005) (upper left), *ii)* mean climate change signal from the RCP8.5 scenarios: 2050-2099 minus the 1956-2005 period in the historical experiments (upper right), *iii)* year-to-year variability as indicated by the standard deviation during the historical period (lower left) and *iv)* ratio of the interannual variance in the future relative to the historical period (lower right).

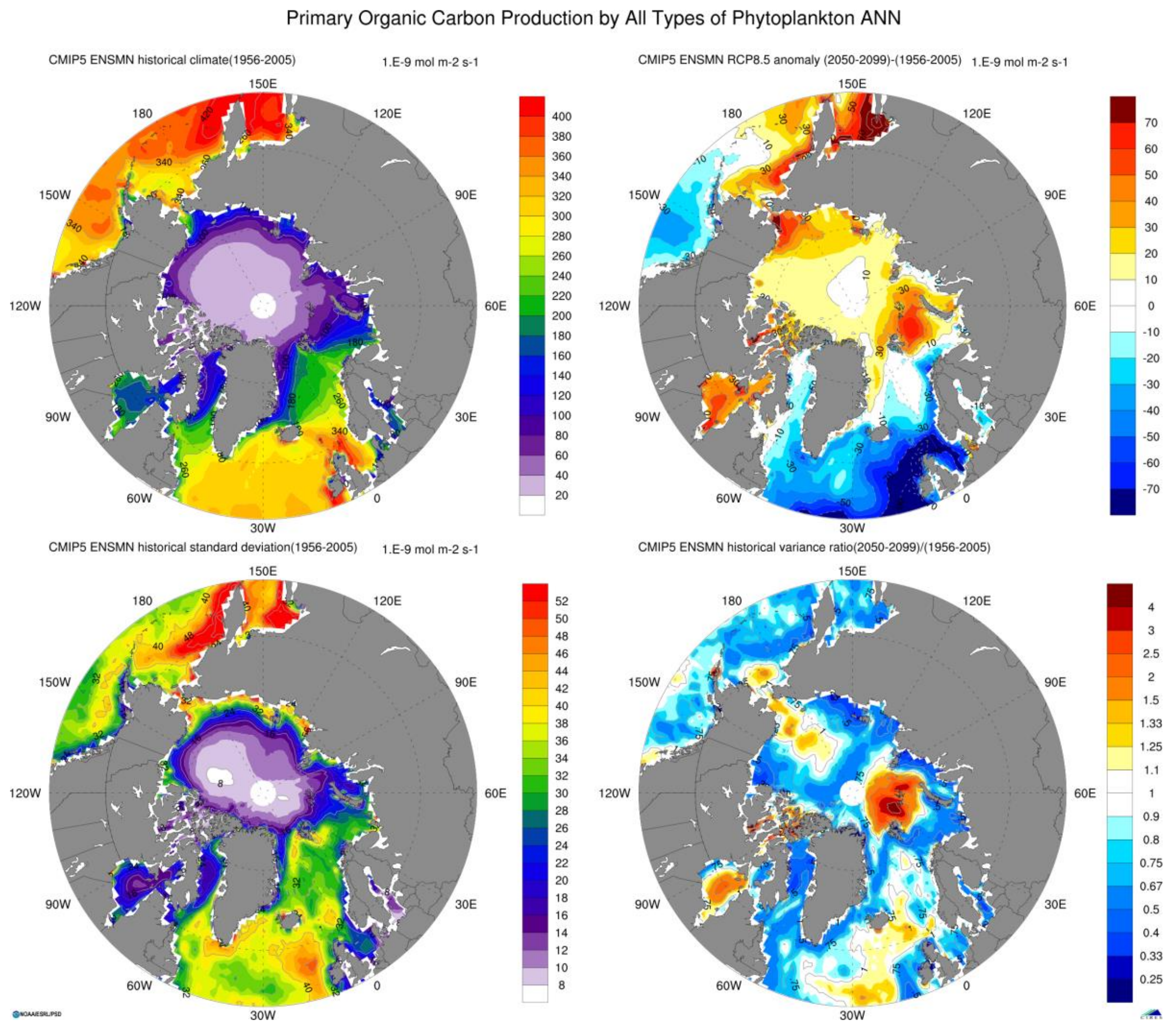

Fig.5: Snapshot from the Ocean and Marine Ecosystems section of the Climate Change Web Portal depicting the CMIP5 ensemble mean Net Primary Productivity of Carbon by Phytoplankton in the top 150m ($1e^{-9}$ mol m^{-2} s^{-1}) for *i)* mean during the historical period (1956-2005) (upper left), *ii)* mean climate change signal from the RCP8.5 scenarios: 2050-2099 minus the 1956-2005 period in the historical experiments (upper right), *iii)* year-to-year variability as indicated by the standard deviation during the historical period (lower left) and *iv)* ratio of the interannual variance in the future relative to the historical period (lower right).